

Theory of Anisotropic Hopping Transport due to Spiral Correlations in the Spin-Glass Phase of Underdoped Cuprates

Valeri N. Kotov¹, and Oleg P. Sushkov^{2,y}

¹ Institute of Theoretical Physics, Swiss Federal Institute of Technology (EPFL),
CH-1015 Lausanne, Switzerland

² School of Physics, University of New South Wales, Sydney 2052, Australia

We study the in-plane resistivity anisotropy in the spin-glass phase of the high- T_c cuprates, on the basis of holes moving in a spiral spin background. This picture follows from analysis of the extended $t-t^0$ model with Coulomb impurities. In the variable-range hopping regime the resistivity anisotropy is found to have a maximum value of around 90%, and it decreases with temperature, in excellent agreement with experiments in $\text{La}_2 \times \text{Sr}_x \text{CuO}_4$. In our approach the transport anisotropy is due to the non-collinearity of the spiral spin state, rather than an intrinsic tendency of the charges to self-organize.

One of the central issues in the physics of the high-temperature superconductors is the nature of the ground state at low doping. In particular, the possible co-existence of ordering tendencies in the spin and charge sectors at low temperature is currently being actively investigated [1, 2, 3]. Experimentally at low temperature $\text{La}_2 \times \text{Sr}_x \text{CuO}_4$ (LSCO) co-doped with Nd (LNSCO) exhibits static lattice deformation [4] as well as incommensurate (IC) magnetism at doping $x = 1/8$. The lattice deformation indicates the presence of static charge order (stripes). Recently similar behavior has also been found in $\text{La}_2 \times \text{Ba}_x \text{CuO}_4$ (LBCO) [5], $x = 1/8$. However for $x < 1/8$ and in Nd-free LSCO charge order has not been detected, while IC magnetism persists down to $x = 0.02$ [6, 7]. Thus while IC magnetism is generically observed in the underdoped regime, static charge order seems to be confined to the neighborhood of $x = 1/8$.

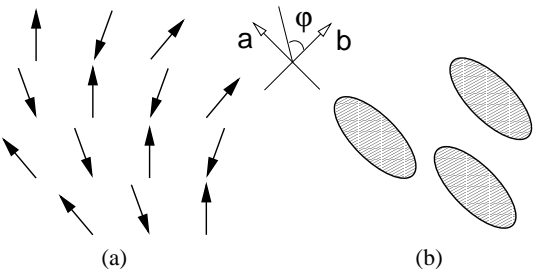


FIG. 1: (a) (1,1) Spiral spin state. (b) Localized (Coulomb trapped) holes, with positions pinned by the random Sr impurities (schematic). The ellipses reflect the symmetry of the wave-function (5). The orthorhombic \hat{a} and \hat{b} directions are shown.

Theoretically the IC magnetism in the cuprates is often modeled as originating from static charge stripes, and since these are not universally present, one is forced to introduce additional concepts, such as "fluctuating" stripes, electronic liquid crystals, etc. [3, 8]. The microscopic origin of such states is still not clear and is currently being debated. An alternative explanation for the IC magnetism which follows naturally from the $t-t^0$

model, is the formation of a non-collinear spiral state, partially relieving the frustration due to the hole motion [9]. Such a state would not co-exist with charge order, as can be shown in the context of the effective Landau theory [10]. However it is still possible that in the presence of anisotropic Dzyaloshinskii-Moriya interactions the spin spiral could cause weak lattice modulation with period generically half that of the spiral. While the spiral ground state has a tendency to be unstable toward phase separation, we have shown recently that in the extended $t-t^0$ model the spiral can be stabilized by the presence of the additional hoppings [11]. The spiral description was successfully applied to explain magnetic properties of LSCO, such as the location of the elastic neutron scattering peaks and the change of the incommensurability direction by 45° across the superconductor-insulator boundary ($x = 0.055$) [12]. The spiral was also proposed as a candidate for the ground state in the spin-glass (insulating) phase for $0.02 < x < 0.055$ [12, 13, 14].

In the present work we address transport properties within the spiral framework. Our main motivation comes from the recent experimental data in the spin-glass phase of LSCO showing transport anisotropies as large as 50% to 70%, both in DC and AC measurements [15, 16]. It has been argued that these data provide indirect support to the notion of fluctuating stripes or electronic liquid crystals, but no quantitative theory exists that takes these concepts into account [3]. Recent infrared experiments that carefully identify phonon modes in LSCO once again find no charge ordering tendencies in the spin-glass phase of this material [17]. Therefore we take the point of view that the ground state has a spiral spin structure, and calculate the transport anisotropy in the variable-range hopping (VRH) regime for low temperature and frequency, where the anisotropy has the largest value. We show that the spatial anisotropy of the hole wave-function in a spiral translates into anisotropy of the hopping transport. Our main result is that for microscopic parameters appropriate for LSCO (within the $t-t^0$ model), the magnitude of the anisotropy is large and close to the one

found experimentally. Thus we demonstrate, for the first time, that the transport anisotropy data can be explained quantitatively within a theory that does not involve any tendency of the holes to self-organize into charge stripes.

Our starting point is the description of the spin-glass phase ($0.02 < x < 0.055$) developed in [12] which is briefly summarized below. First, a single hole resides near the points $k_0 = (1=2, 2=2)$, with a quadratic dispersion around them $k = \frac{1}{2}k_1^2 + \frac{2}{2}k_2^2$, where k_1 is perpendicular to the face of the magnetic Brillouin zone and k_2 is parallel to the face. Within the effective $t = t^0$ J model for LSCO, the parameters are taken to be: $t=J = 3.1$; $t^0=J = 0.5$; $t=J = 0.3$, where $J = 125$ meV. From now we measure energies in units of J (i.e. set $J = 1$) and lengths in units of the lattice spacing a (we set $a = 1$). The parameters lead to an almost isotropic dispersion $k_1^2 + k_2^2 = 2.2$, and a quasiparticle residue around the nodal points $Z = 0.34$. A hole trapped by the Coulomb field of the Sr ion generates a spiral distortion of the Néel background, which can be parameterized as: $j_{ii} = e^{i(k_1)m} - 2j''i$; $j_{jj} = e^{i(k_2)m} - 2j''j$, i 1/2 "up" sublattice; j 2 "down" sublattice, where m is an arbitrary unit vector perpendicular to the quantization axis of the states $j''i$, $j''j$. The angle (r) measuring deviations from collinearity is given by [12]:

$$\chi(r) = \frac{Zt}{2s} \frac{(e-r)}{r^2} \left[1 - e^{2r} (1 + 2r) \right]; \quad (1)$$

where $s = 0.18$ is the spin stiffness, and $1 = 3.5$ is the localization length of the orbital part of the wave function. The value of $1 = 3.5$ is extracted from experimental data [12], and is generally expected to increase with doping. The unit vector $e = \frac{1}{2}(1, 1)$, in the usual square-lattice coordinate system. At finite doping ($0.02 < x < 0.055$) the interaction of the long-range dipole distortions from holes trapped at different Sr ions leads to spiral magnetic order [12], characterized by average $\langle e \cdot r \rangle$, as shown in Fig 1(a). In a perfect square lattice the spiral can be directed along any diagonal (1, 1). However from the location of the elastic neutron scattering peaks [6] the incommensurability is determined to be along the orthorhombic \hat{b} direction. In our picture this means that the orthorhombic deformation pins the direction of the spiral, as shown in Fig. 1, and thus we set $e = e_+ = \frac{1}{2}(1, 1)$. In what follows the exact nature of the pinning mechanism, to be discussed elsewhere, will not be important.

Experimentally the magnetic correlation length is finite $\sim 6-20$ (decreases with increasing doping) [6, 7]. On the theoretical side it was argued that \sim is finite due to topological defects that lead to frustration of the long-range spiral order [12, 13]. Since the localization length is less than the magnetic scale, $1 = \sim$, we expect that the effective description of transport properties, developed below in terms of the one-hole wave function, is quanti-

tatively valid also at finite (small) doping (i.e. the topological frustration mechanism does not affect our considerations).

Localized hole in the presence of magnetic spiral correlations. The coupling between the spin of the magnetic background (angle (r)) and the orbital wave-function of the hole (r) generates the spiral and has the form [12]: $H_{SP} = \frac{p^2}{2Zt} (e \cdot r) \varphi(r) d^2r$. The effective Schrödinger equation is then:

$$\frac{-r^2}{2} \frac{q^2}{r} \frac{p^2}{2Zt(e \cdot r)} \chi(r) = \chi(r); \quad (2)$$

Here the Coulomb potential of the Sr ion which keeps the hole localized is $\frac{q^2}{r} = \frac{q_0^2}{E_e r}$, where q_0 is the unit charge and E_e is the effective dielectric constant known to be quite large in the copper oxides, $E_e \sim 30-100$ (increases with doping) [18]. The last term in (2) determines the

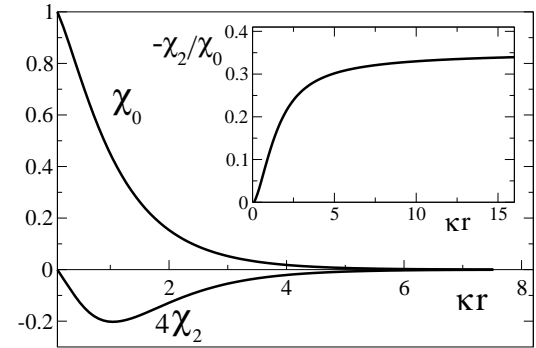


FIG. 2: Solution of (2) in terms of the expansion (5), for $s = 1$: Only the first two (largest) components are shown. The normalization of χ_0 is arbitrary. Inset: The ratio $-\chi_2/\chi_0$.

anisotropy $\chi(r)$ and is given by

$$\frac{p^2}{2Zt(e \cdot r)} = \frac{Z^2 t^2}{s} \frac{1}{r^2} [f(r) - g(r) \cos(2\theta)];$$

$$g(z) = 1 - (1 + 2z + 2z^2)e^{-2z}; \quad f(z) = 2z^2 e^{-2z}; \quad (3)$$

The coordinate system is chosen so that e is parallel to the \hat{b} axis and θ is the polar angle (Fig. 1). The value of θ (and consequently χ) can be found by a variational minimization of the total energy [12]:

$$= \frac{2q^2}{1-2}; \quad = \quad 2=2; \quad \frac{Z^2 t^2}{s}; \quad (4)$$

We will use $\theta = 0.3-0.4$, consistent with experiment [12], rather than rely on (4) which contains the uncertainty related to the exact value of the dielectric constant. The dimensionless parameter θ , as defined in (4), characterizes the coupling between the orbital motion of the hole and the deformation of the spin background. The numerical value is ~ 1 , appropriate for LSCO, which will

be used from now on. Let us look for solution of (2) in term s of the series in angular harmonics

$$(\mathbf{r};') = \rho_0(\mathbf{r}) + \rho_2(\mathbf{r}) \cos(2\theta') + \rho_4(\mathbf{r}) \cos(4\theta') + \dots \quad (5)$$

Then Eq. (2) leads to a set of coupled equations for ρ_i ; $i = 0, 2, 4, \dots$. We have solved these equations numerically and the results for the first two harmonics are presented in Fig. 2. The next harmonics are found to be small, for example $\rho_4 = \rho_0 < 2 \times 10^{-2}$, and can be in fact safely neglected. At large distances all the wave-functions behave as $1/e^r$, while at finite distances this behavior is substantially modified, as shown in Fig. 2.

DC transport anisotropy in the variable-range hopping (VRH) regime. Below characteristic temperature $T_{VRH} \approx 20-30K$, the low-temperature resistivity of LSCO in the spin-glass phase can be described by the 2D version of the Mott VRH formula $\rho = \exp(T_0/T)^{1/3}$ [18, 19, 20, 21]. Here T_0 depends somewhat on doping and sample quality. For example at 4% doping the data of [19] are well fitted with $T_0 = 500K$ [20]; analyzing the curves of [21] we obtain $T_0 = 200-300K$, and from [15] we have extracted $T_0 = 200K$.

Within the spiral framework the physical idea behind the resistivity anisotropy is quite simple. According to (5) the hole wave function acquires an elliptic deformation induced by the spin spiral, as shown schematically in Fig. 1(b). Hence hopping in the \hat{b} -direction is less probable than hopping in the \hat{a} -direction. Using (5), and essentially following the derivation of Mott's result [22], we obtain for the resistivity anisotropy:

$$\frac{\rho_b(T)}{\rho_a(T)} = \frac{\int_0^{R_2} \sin^2(\theta') \rho^2(r_T; \theta') d\theta'}{\int_0^{R_2} \cos^2(\theta') \rho^2(r_T; \theta') d\theta'}; \quad (\mathbf{r};') = \frac{\rho_0(\mathbf{r})}{\rho_0(\mathbf{r})}$$

Here $r_T = \frac{1}{2}(T_0/T)^{1/3}$ is the VRH length [22], and in order for the approach to be justified we must certainly have $r_T > 1$. It is clear from (6) that as T decreases (i.e. r_T increases) the anisotropy grows, due to the increase of ρ_b/ρ_a (Fig. 2 (Inset)) and consequently the more pronounced angular dependence of $\rho(r_T; \theta')$. The results are summarized in Fig. 3, where also the evolution of the zero-temperature anisotropy $\rho_b(T=0)/\rho_a(T=0)$ as a function of Λ is shown for completeness in the inset. At very low temperature ($T < 1K$ [20], i.e. $T=T_0 < 10^{-3}$) we would have to take into account a crossover to the Coulomb gap regime, which however would practically not influence the curve in Fig. 3.

The data of [15] were taken at temperatures $T > 10K$, meaning that the lowest ratio $T=T_0 = 0.05$ (we take $T_0 = 200K$). As the temperature increases beyond $T_{VRH} \approx 20-30K$ when $\Lambda \approx 1$ the approach based on VRH conduction ceases to be valid, as the conduction mechanism changes to impurity band conduction and eventually quasimetallic behavior. In the most relevant low-temperature range below T_{VRH} (corresponding

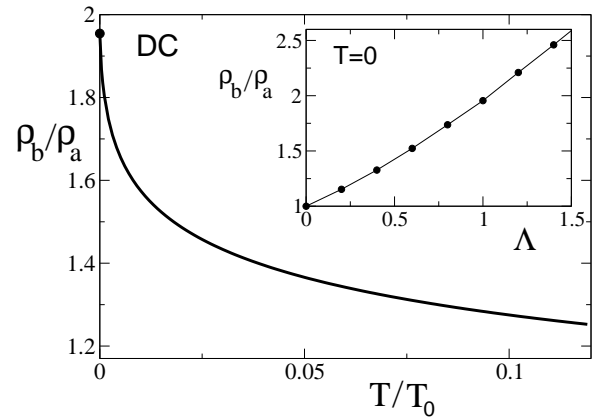


FIG. 3: DC resistivity anisotropy in the VRH regime, for $\Lambda = 1$. Inset: Maximum ($T = 0$) anisotropy versus Λ .

to largest anisotropy), both the calculated magnitude of ρ_b/ρ_a and its temperature dependence are very close to the experimental results [15], although in these experiments the temperature is not low enough to penetrate the "deep" VRH regime $T=T_0 < 0.05$ where the anisotropy should increase even further. It should be also noted that there exists quite a bit of uncertainty in the determination of T_0 and hence in the determination of the exact value of ρ_b/ρ_a from Fig. 3.

AC transport anisotropy in the VRH regime. At finite frequency and temperature the calculation of the AC conductivity is a very complicated problem. However in the "quantum" limit when the frequency $\omega \ll T$, the VRH AC conduction is expected to be dominated by resonant absorption by singly occupied pairs (without involvement of phonons), and is usually relevant in doped semiconductors [23]. The VRH length in the AC regime (neglecting for a moment the angular dependence of the states) is logarithmic [23]: $r_T = (1/\omega) \ln(2j_f + 1)$, which is the main difference from the DC case. From now on we denote $\omega = (2j_f)^{1/2}$. The functional dependence of the conductivity in 2D at low frequency $\ln(1/\omega) \ll 1$ is given by the Mott-Efros-Shklovskii expression: $\sigma(\omega) = \sigma_0 \ln(1/\omega) + \sigma_1 \omega^2 = r_T^2 [1 + \omega^2/r_T^2]$, where the second term takes into account the Coulomb interaction in the resonant pair [23]. The generalization of the Mott-Efros-Shklovskii formula to the anisotropic case is straightforward: one needs to replace $\ln(1/\omega)$ by $L = \ln(\rho(r_T; \theta'))$, where $\rho(r_T; \theta')$ is defined in (6). Hence we obtain for the resistivity anisotropy:

$$\frac{\rho_b(\omega)}{\rho_a(\omega)} = \frac{\int_0^{R_2} \sin^2(\theta') \rho^2(r_T; \theta') d\theta'}{\int_0^{R_2} \cos^2(\theta') \rho^2(r_T; \theta') d\theta'}; \quad (7)$$

$$\rho(r_T; \theta') = L^2 \left(1 + \frac{2}{1 + \omega^2 L^2} \right)^{-1/2}$$

The expression (7) is plotted in Fig. 4. Due to the logarithmic dependence, in the theoretical limit of zero frequency the anisotropy would vanish (albeit very slowly),

ie. $\rho_b(\omega = 0) = \rho_a(\omega = 0) = 1$. However one must keep in mind that the above expressions are not valid at arbitrary low frequencies, as we must have $\omega > T$. Generally we find that the (maximum) AC anisotropy of 30–40% is somewhat smaller than the DC anisotropy.

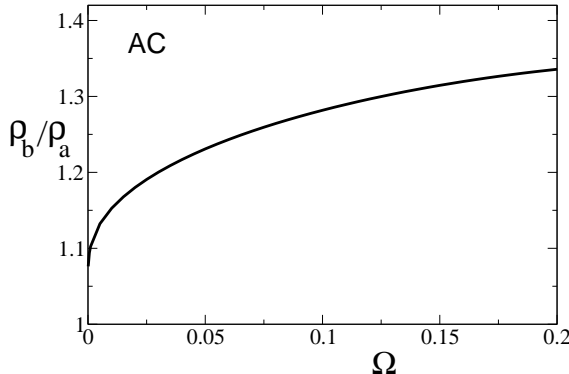


FIG. 4: AC VRH resistivity anisotropy versus $\omega = \Omega(2j)$ in the regime $T < \omega$, and $\ln(1/\omega) < 1$, for $\omega = 1$.

When attempting to compare our results to the experimental data of [16] we realize that ω and T are not sufficiently low, nor is the difference between them sufficiently high to justify the separation into "quantum" and "thermal" VRH conduction and consequently the Mott-Efros-Shklovskii approach. The temperature used is $T = 13$ K and at the lowest frequency of $\omega = 20$ cm⁻¹ = 2.5 m eV, estimating for the hole energy $j = j_0 = 2 = 5 = 10$ m eV, we have $0.13 = 0.25$. Moreover, upon increasing the frequency to $80 = 100$ cm⁻¹, a change of behavior from insulating to conducting takes place, a broad peak develops [16], and consequently it is not clear to us that the AC data are ever in a clean VRH regime. In spite of all this the magnitude of the calculated anisotropy agrees reasonably well with experiment. It should be experimentally possible to lower T (towards the mK range) as well as ω in order to probe the VRH AC anisotropy more reliably and compare with our theory.

We would like to reiterate that in our theory there is no tendency of the holes to form charge stripe-like structures. Nevertheless the resistivity shows anisotropic behavior (and so does the uniform magnetic susceptibility, to be discussed separately). The present work is relevant to the spin-glass regime of $\text{La}_{2-x}\text{Sr}_x\text{CuO}_4$, $0.02 < x < 0.055$. However we have also argued [11, 12] that the spin spiral structure could exist in the superconducting state $x > 0.055$. The theory naturally explains why the incommensurate direction, determined from elastic neutron scattering, rotates by 45° exactly at the insulator-superconductor transition point. On the other hand it is usually argued that at $x = 1 = 8$ both in charge-ordered LNSCO [4] and LBCO [24], non-collinear spiral order is not consistent with experiment. We would

indeed not claim that spiral ground state is stable at that particular doping since in fact the spiral becomes commensurate with the lattice and therefore significant changes in the ground state could occur due to the spin-lattice coupling.

In conclusion, starting from a spiral ground state which unambiguously follows from the extended t-J model, we have calculated the in-plane anisotropy of the low-temperature DC and low-frequency AC resistivity of $\text{La}_{2-x}\text{Sr}_x\text{CuO}_4$ in the spin-glass phase. The theory has no fitting parameters and the calculations are performed for the variable-range hopping regime. Within the spiral description the transport anisotropy is due to the anisotropy of the hole wave-function since the hole hops in a non-collinear (spiral) spin background. The AC anisotropy reasonably agrees with experiment in spite of the fact that the data are on the border of the VRH regime. The experimental data for the DC resistivity are well within the VRH regime and here both the calculated magnitude and temperature dependence of the anisotropy agree with experiment very well.

We are grateful to L. Benfatto, J. Haase, and D. Poilblanc for valuable discussions and comments. The support of the Swiss National Fund is acknowledged (V.N.K.).

Electronic address: valerikotov@ep.ch
^y Electronic address: sushkov@phys.unsw.edu.au

[1] K.O. renstein and A.J. Millis, *Science* 288, 468 (2000).
[2] S. Sachdev, *Rev. Mod. Phys.* 75, 913 (2003).
[3] S.A.Kivelson et al., *Rev. Mod. Phys.* 75, 1201 (2003).
[4] J.M.Truanquada et al., *Phys. Rev. B* 54, 7489 (1996).
[5] M.Fujita et al., *Phys. Rev. B* 70, 104517 (2004).
[6] S.Wakimoto et al., *Phys. Rev. B* 61, 3699 (2000); M. Matsuda et al., *Phys. Rev. B* 62, 9148 (2000).
[7] M.Fujita et al., *Phys. Rev. B* 65, 064505 (2002).
[8] S.A.Kivelson, E.Fradkin, and V.J.Emery, *Nature* 393, 550 (1998).
[9] B.I.Shraiman and E.D.Siggia, *Phys. Rev. Lett.* 62, 1564 (1989); *Phys. Rev. B* 42, 2485 (1990).
[10] O.Zachar, S.A.Kivelson, and V.J.Emery, *Phys. Rev. B* 57, 1422 (1998).
[11] V.N.Kotov and O.P.Sushkov, *Phys. Rev. B* 70, 195105 (2004), and cited references.
[12] O.P.Sushkov and V.N.Kotov, *Phys. Rev. Lett.* 94, 097005 (2005).
[13] N.Hasselman, A.H.Castro Neto, and C.Moraes Smith, *Phys. Rev. B* 69, 014424 (2004).
[14] V.Juricic et al., *Phys. Rev. Lett.* 92, 137202 (2004).
[15] Y.Ando et al., *Phys. Rev. Lett.* 88, 137005 (2002).
[16] M.Dumm et al., *Phys. Rev. Lett.* 91, 077004 (2003).
[17] W.J.Padilla et al., cond-mat/0505094.
[18] M.A.Kastner et al., *Rev. Mod. Phys.* 70, 897 (1998).
[19] B.Kemper et al., *Phys. Rev. B* 46, 14034 (1992).
[20] E.Lai and R.J.Goding, *Phys. Rev. B* 57, 1498 (1998).
[21] M.Suzuki, *Phys. Rev. B* 39, 2312 (1989).
[22] N.F.Mott and E.A.Davis, *Electronic Processes in Non-*

Crystalline Materials, 2-nd ed. (Clarendon Press, Oxford, 1979).

[23] A. L. Efros and B. I. Shklovskii, in *Electron-Electron Interactions in Disordered Systems*, edited by A. L. Efros and M. Pollak, p. 409 (North-Holland, Amsterdam, 1985).

[24] M. Hucker, G. D. Gu, and J. M. Tranquada, cond-mat/0503417.